

# Violation of the Pauli-Clogston limit in a heavy Fermion superconductor CeRh<sub>2</sub>As<sub>2</sub> –Duality of itinerant and localized 4f electrons–

Kazushige Machida

*Department of Physics, Ritsumeikan University, Kusatsu 525-8577, Japan*

(Dated: July 12, 2022)

We theoretically propose a mechanism to understand the violation of the Pauli-Clogston limit for the upper critical field  $H_{c2}$  observed in the Ce bearing heavy Fermion material CeRh<sub>2</sub>As<sub>2</sub> from the view point of spin singlet pairing. It is based on a duality concept, the dual simultaneous aspects of an electron: the itinerant part and localized part of quasi-particles (QPs) originated from the 4f electrons of the Ce atoms. While the itinerant QPs directly participate in forming the Cooper pairs, the localized QPs exert the internal field so as to oppose the applied field through the antiferromagnetic exchange interaction between them. This is inherent in the dense Kondo lattice system in general. We argue that this mechanism can be applied not only to the locally noncentrosymmetric material CeRh<sub>2</sub>As<sub>2</sub>, but also to globally inversion symmetry broken Ce-based materials such as CePt<sub>3</sub>Si. Moreover, we point out that it also works for strongly Pauli limit violated spin triplet pairing systems, such as UTe<sub>2</sub>.

PACS numbers: 74.70.Tx, 74.20.-z, 74.25.-q

## I. INTRODUCTION

The newly found heavy Fermion superconductor (SC) CeRh<sub>2</sub>As<sub>2</sub> is attracting enormous attention both experimentally<sup>1–5</sup> and theoretically<sup>6–13</sup> because, compared with the SC transition temperature  $T_c=0.35\text{K}$  both of the upper critical fields  $H_{c2}^c \sim 16\text{T}$  for the  $c$ -axis and  $H_{c2}^{ab} \sim 2\text{T}$  for the  $ab$ -plane exceed the Pauli-Clogston limit estimated by the weak coupling BCS formula  $H_P^{\text{BCS}} = 1.84T_c \sim 0.6\text{T}$  in the tetragonal crystal symmetry. The degree of the violation of the Pauli limit  $H_{c2}^c/H_P^{\text{BCS}} \sim 27$  is extraordinary.

Given that the local symmetry on the Ce sites breaks the inversion symmetry, it is argued that the spin singlet-triplet mixing scenario to overcome the Pauli limitation is realized in this compound<sup>6–13</sup>. This scenario is an extended version designed for globally noncentrosymmetric SC materials<sup>14–20</sup>, in particular on Ce heavy Fermion SC<sup>21</sup> such as CePt<sub>3</sub>Si<sup>22–25</sup>, CeIrSi<sub>3</sub><sup>26,27</sup>, CeRhSi<sub>3</sub><sup>28</sup>, and CeCoGe<sub>3</sub><sup>29</sup>. They also break the Pauli limitation and CeIrSi<sub>3</sub> exhibits a record high  $H_{c2} \sim 45\text{T}$  with  $T_c=2\text{K}$  under pressure<sup>28</sup>. However, no firm experimental evidence has proven those theories so far.

There have been several known mechanisms to explain the Pauli limit violation apart from the spin triplet pairing. For example, the Fulde-Ferrell-Larkin-Ovchinnikov (FFLO) state can raise the Pauli limit, but it is only within a factor of 2 or so of  $H_{c2}^c/H_P^{\text{BCS}}$  at most<sup>30</sup>. An especially designed thin film system with few layers shows the enhanced  $H_{c2}$  due to strong spin-orbit coupling, leading to the so-called Ising superconductivity<sup>31,32</sup>, or twisted magic angle graphene exhibits also the Pauli limit violation<sup>33</sup>. Apparently, those are not appropriate for the present three dimensional bulk systems.

To understand the strong Pauli limit violation in CeRh<sub>2</sub>As<sub>2</sub>, the following should be noted:

(1) The phase diagram in  $H(\parallel c)$  vs  $T$  is subdivided into the SC1 and SC2 phases<sup>1</sup> for low and high fields sepa-

rated by a first order line at  $H=4\text{T}$  as shown schematically in Fig. 1(a). The SC2 phase reaches 16T far beyond the Pauli limit with a large margin as mentioned.

(2) Below  $T_c=0.35\text{K}$ , the antiferromagnetic order (AF) develops at  $T_N=0.25\text{K}$  whose detailed AF structure has not been determined yet<sup>34,35</sup>. This order disappears above the field  $H^c > 4\text{T}$  applied along the  $c$ -axis<sup>36</sup>, whose value approximately coincides with the SC1 and SC2 boundary line.

(3) By tilting the field direction from the  $c$ -axis towards the  $ab$  plane by the angle  $\theta$ , the enhanced  $H_{c2}(\theta)$  quickly diminishes up to  $\theta \sim 30^\circ$  beyond which  $H_{c2}(\theta)$  smoothly tends to  $H_{c2}^{ab}=2\text{T}$  for the  $ab$ -plane<sup>3</sup>. Thus, the low field phase of the SC1, starting below 4T for the  $c$ -axis, is continuously connected to  $H_{c2}^{ab}$ .

(4) According to the recent Knight shift (KS) experiments of <sup>75</sup>As-NMR by the Ishida group<sup>34–36</sup>, not only for the SC1 phase, but also for the SC2 phase for the  $c$ -axis, KS does decrease below  $T_c$ , negating a spin triplet phase. Note that KS also decreases for the  $ab$ -plane field<sup>37</sup>. There is evidence neither for the spin-triplet pairing, nor the singlet-triplet mixing associated with local inversion symmetry breaking<sup>6–13</sup>. This urges us to consider the Pauli limit violation within the spin-singlet framework, or more broadly a framework applicable to both singlet and triplet pairings.

(5) It is noteworthy to remind of the fact that LaRh<sub>2</sub>As<sub>2</sub><sup>38</sup> with identical locally non-centrosymmetric crystal structure and similar  $T_c \sim 0.3\text{K}$ , shows neither the enhanced  $H_{c2}$  ( $H_{c2}^c=10\text{mT}$  and  $H_{c2}^{ab}=12\text{mT}$ ), nor the multiple phase diagram. This means that the 4f electrons of the Ce atoms play crucial roles in those intriguing phenomena, in particular the strong Pauli limit violation of  $H_{c2}^c = 16\text{T}$ .

(6) Substantial magnetic moments are progressively induced with increasing applied fields at low  $T$ , i.e.,  $M_c(M_{ab})=0.2$  (0.4)  $\mu_B/\text{Ce}$  for the  $c$  ( $ab$ )-axis under  $H=15\text{T}$ . In view of the dual nature of the 4f electrons

of the Ce atoms in the present dense Kondo lattice material with  $T_{\text{Kondo}} \sim 30\text{K}$ , a part of the 4f electrons is localized to form the AF order and the other part is itinerant to form a coherent Fermion state with heavy quasi-particle mass; It has a huge Sommerfeld coefficient  $\gamma_{\text{N}} \sim 1\text{J/mol}\cdot\text{K}^2$ . The latter directly participates in the Cooper pair formation. This duality or dichotomy of the 4f electrons is essential in unveiling the physics of  $\text{CeRh}_2\text{As}_2$ .

All figures are schematic throughout the paper, intending to no quantitative meaning.

## II. BASIC IDEA AND ASSUMPTIONS

To overcome the fundamental and seemingly unavoidable  $H_{c2}$  limitation due to the Pauli paramagnetic effect associated with a spin singlet pairing, we consider the effects of the localized moment  $M(H)$  originating from the 4f electrons on the Ce atomic sites. This is to exert the internal field  $J_{\text{cf}}M(H)$  to the conduction electrons through the c-f exchange interaction  $J_{\text{cf}}$  coming from the periodic Kondo lattice Hamiltonian necessary for describing the heavy Fermion systems in general. In the past, this interaction was considered to play several important and crucial roles in the coexistence problems of magnetism and superconductivity. In the ferromagnetic case, it stabilizes the FFLO state via the ferromagnetic molecular field<sup>39</sup> whereas in the AF case, it yields the suppressed  $H_{c2}$  below  $T_{\text{N}}$ <sup>40–42</sup>. This idea is somewhat similar to the Jaccarino-Peter mechanism<sup>43</sup>.

The sign of  $J_{\text{cf}} > 0$  is generically antiferromagnetic for our dense Kondo lattice systems, i.e.,  $\text{CeRh}_2\text{As}_2$ , to realize the Kondo effect which ultimately leads to the heavy Fermion phenomenology. Thus, the effective internal field  $H_{\text{eff}}$  felt by the conduction electrons is written as

$$H_{\text{eff}}(H) = H - J_{\text{cf}}M(H), \quad (1)$$

with  $H$  being the applied external field. We assume that in the AF order, the sublattice moment is parallel to the  $c$ -axis although we know that the system is a magnetically easy  $ab$  plane XY type<sup>35</sup>. This conflicting situation sometimes happens in other Ce-Kondo materials<sup>44</sup>. Under the field parallel to the  $c$ -axis, via a first order transition, the AF flips the moment  $M_0$  towards the  $c$ -axis at  $H_{\text{FL}}$  in general. We assume  $H_{\text{FL}}=4\text{T}$ , coinciding with the field above in which the NMR experiment detects no AF. Until this spin flop transition  $H < H_{\text{FL}}=4\text{T}$  the total moment  $M(H)=0$  in the normal state. The magnetization process along the  $c$ -axis is schematically depicted in Fig. 1(b) where at  $H_{\text{FL}}=4\text{T}$ , the moment jumps by  $M_0$ . Thus, for the  $c$ -axis,

$$\begin{aligned} M_c(H) &= 0 && \text{for } H < H_{\text{FL}} \\ &= M_0 + \chi_c H + \chi_c^{(3)} H^3 && \text{for } H \geq H_{\text{FL}} \end{aligned} \quad (2)$$

while for the  $ab$ -axis,

$$M_{ab}(H) = \chi_{ab} H + \chi_{ab}^{(3)} H^3 + \dots, \quad (3)$$

where  $\chi_i$  and  $\chi_i^{(3)}$  ( $i = c$  and  $ab$ ) are the linear and non-linear magnetic susceptibilities respectively. By substituting  $M(H)$  into Eq. (1), we obtain

$$\begin{aligned} H_{\text{eff}}^c &= H && \text{for } H < H_{\text{FL}} \\ &= (1 - \chi_c J_{\text{cf}}^c) H - J_{\text{cf}}^c (M_0 + \chi_c^{(3)} H^3) && \text{for } H \geq H_{\text{FL}}. \end{aligned} \quad (4)$$

For  $H \parallel ab$ ,

$$H_{\text{eff}}^{ab}(H) = (1 - \chi_{ab} J_{\text{cf}}^{ab}) H - J_{\text{cf}}^{ab} \chi_{ab}^{(3)} H^3 + \dots. \quad (5)$$

The cf-exchange interaction constants are anisotropic, i.e.,  $J_{\text{cf}}^c \neq J_{\text{cf}}^{ab}$  in general. The following can be clearly observed:

- (1) The external field is scaled by a factor  $1 - \chi J$  as expressed in Eqs. (4) and (5).
- (2) The external field is reduced (enhanced) by a factor  $JM_0$  for the antiferromagnetic  $J_{\text{cf}} > 0$  (ferromagnetic  $J_{\text{cf}} < 0$ ) cf-coupling case, as expressed in Eq. (4).

## III. GL THEORY

### A. $H \parallel c$

To see the effects of the scaling factor and the reduction for the external field on  $H_{c2}$ , we employ the Ginzburg-Landau(GL) theory given by

$$H_{c2}(T) = \alpha_0 \cdot (T_{c0} - T), \quad (6)$$

where the GL coefficient  $\alpha_0 (> 0)$  related to the effective mass determines the slope of  $H_{c2}(T)$  at  $T_{c0}$ . With the effective field  $H_{\text{eff}}$  in place of  $H$  in Eq. (6),  $H_{\text{eff},c2}(T) = \alpha_0 \cdot (T_{c0} - T)$  is obtained. After plugging Eq. (4) into it, we find for  $H \parallel c$

$$\begin{aligned} H_{c2}^c(T) &= \alpha_0^c \cdot (T_{c0} - T) && \text{for } 0 < H < H_{\text{FL}} \\ &= \frac{\alpha_0^c}{1 - \chi_c J_{\text{cf}}^c} \cdot (T_c - T) && \text{for } H \geq H_{\text{FL}} \end{aligned} \quad (7)$$

with

$$T_c = T_{c0} + \frac{J_{\text{cf}}^c}{\alpha_0^c} M_0. \quad (8)$$

Two factors raise  $H_{c2}^c(T)$ , one through the effective mass and the other through  $T_c$ . From now on we neglect the non-linear susceptibility  $\chi^{(3)}$  term for simplicity. For  $H \parallel ab$ , we find

$$H_{c2}^{ab}(T) = \frac{\alpha_0^{ab}}{1 - \chi_{ab} J_{cf}^{ab}} \cdot (T_{c0} - T). \quad (9)$$

We show a schematic  $H_{c2}^c(T)$  in Fig. 1(a). As can be observed from this, when  $H_{c2}^c(T)$  started from  $T_{c0}$  with the slope  $dH_{c2}^c(T)/dT = -\alpha_0^c$  reaches  $H = H_{FL}$ , it jumps by  $J_{cf}^c M_0$  which is estimated by  $\sim 4T$  later. Then, according to Eq. (7),  $H_{c2}^c(T)$  is enhanced by the scaling factor, namely

$$H_{c2}^c(T=0) = \frac{\alpha_0^c T_c}{1 - \chi_c J_{cf}^c}, \quad (10)$$

with the enhanced slope

$$\frac{dH_{c2}^c}{dT} = -\frac{\alpha_0^c}{1 - \chi_c J_{cf}^c}. \quad (11)$$

Notice that the high field part of  $H_{c2}^c(T)$  has the enhanced  $T_c$  given in Eq. (8). Those factors compound to push  $H_{c2}$  to a higher field.

There is no distinction between the SC1 phase for  $0 < H < H_{FL}$  and the SC2 phase for  $H > H_{FL}$  in the pairing symmetry in our scenario. Note, however, that the SC1 phase coexists with AF below  $T_N$ . Various observed thermodynamic anomalies<sup>1</sup> at  $H=4T$  such as ac-susceptibility  $\chi_{ac}(H)$ ,  $M_c(H)$ , and magnetostriction are due to the first order phase transition associated with the AF spin flop transition  $H_{FL}$  although it was interpreted as the pairing symmetry change from a spin singlet to triplet pairing<sup>1-3,38</sup>.

In Fig. 1(b) we illustrate the magnetization curves both for the SC and normal states. At  $H = H_{FL}$  vis the first order spin flop transition  $M_c(H)$  exhibits a jump by  $M_0$  in the normal state. Correspondingly, in the SC state a negative jump by  $-J_{cf}^c M_0$  appears. According to the data<sup>1</sup>, the magnetization curve exhibits a kink-like anomaly at  $H=4T$  in the superconducting state. We interpret it as a first order negative jump.

As shown later, the SC1 phase is strongly suppressed by the Pauli paramagnetic effect characterized by a large Maki parameter, compared with the SC2 phase. The Sommerfeld coefficient  $\gamma(H)$  exhibits a characteristic downward curvature<sup>46,47</sup> up to  $H < H_{FL}$  as displayed in Fig. 1(c). This is followed by a plateau corresponding to the  $H_{c2}$  jump above which  $\gamma(H)$  grows slowly and monotonically. The existing data<sup>4</sup> for  $\gamma(H)$  and thermal conductivity  $\kappa(H)$  at the lowest temperature limit both exhibit a similar behavior. Those data are consistent with the above picture.

In Fig. 1(d) we summarize the field evolution of effective field  $H_{eff}(H)$ ; For  $H < H_{FL}$ ,  $H_{eff}(H) = H$ . Then after showing the negative jump of  $-J_{cf}^c M_0$ , it grows linearly up to  $H_{c2}$  where  $H_{eff} = \alpha_0^c T_{c0}$ . This value is far less than the reached  $H_{c2}^c(T=0)$  given by Eq. (10).

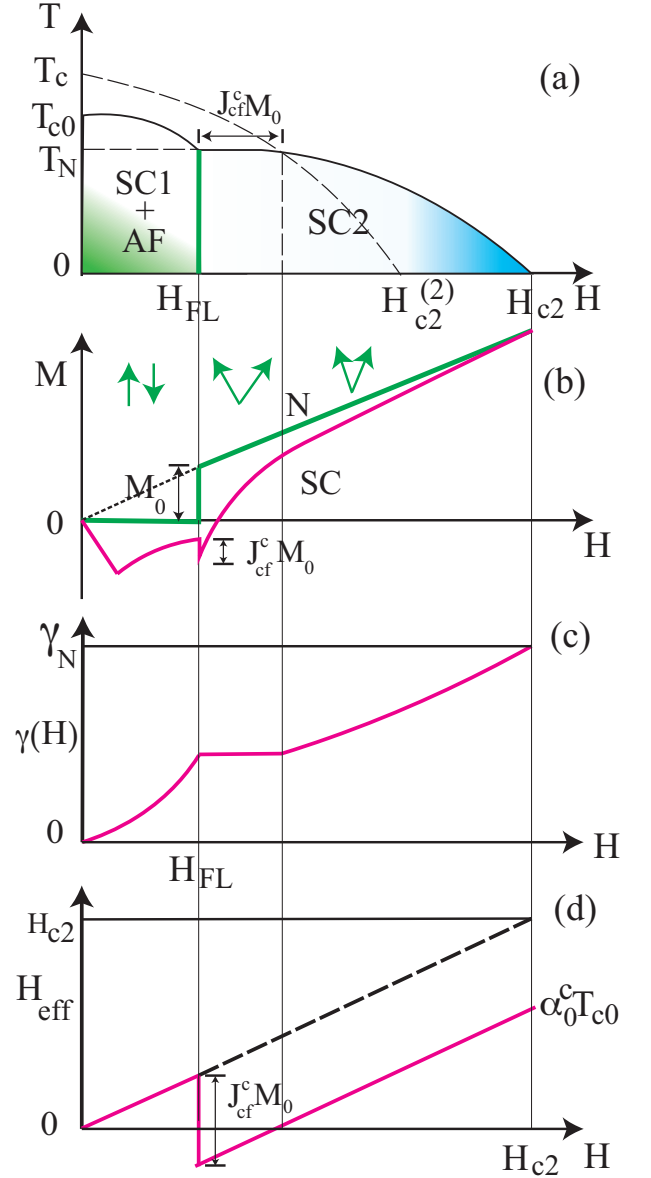


FIG. 1: The field dependences of various quantities for  $H||c$ -axis. (a)  $H_{c2}$  vs  $T$  phase diagram. SC1 starts at  $T_{c0}$  with the slope  $dH_{c2}/dT = -\alpha_0^c$  and reaches  $\alpha_0^c T_{c0}$  at  $T=0$ .  $H_{c2}^{(2)} = \alpha_0^c (T_c - T)$  for SC2.  $H_{c2}$  ultimately reaches  $\alpha_0^c T_{c0} / (1 - J_{cf}^c \chi_c)$  at  $T = 0$  with the enhanced slope  $-\alpha_0^c / (1 - J_{cf}^c \chi_c)$ . Note a jump by  $J_{cf}^c M_0$ . (b) Magnetization processes for the normal (N) and SC states. In the normal state  $M=0$  for  $H < H_{FL}$  and jumps by  $M_0$  at  $H_{FL}$  via the first order spin flop transition. In the SC it exhibits the negative jump by  $-J_{cf}^c M_0$  on top of SC diamagnetic background. Here we sketch the AF spin configurations for each field region where at  $H = 0$  the moment points to the  $c$  direction. (c) Field dependence of  $\gamma(H)$ . In SC1 for  $0 < H < H_{FL}$  it shows a strong Pauli affected curve with a concave curvature<sup>47</sup>. Corresponding to the  $H_{c2}$  jump,  $\gamma(H)$  stays a constant and then gradually increases up to the normal value  $\gamma_N$  at  $H_{c2}$ . (d) The effective field  $H_{eff}(H) = H$  for  $0 < H < H_{FL}$ . After showing the negative jump by  $-J_{cf}^c M_0$ ,  $H_{eff}(H)$  grows linearly in  $H$  and reaches  $\alpha_0^c T_{c0}$  at  $H_{c2}$  far below the un-enhanced case drawn by the dashed line.

## B. $H\parallel ab$

Let us consider the case of  $H\parallel ab$  whose direction is perpendicular to the AF moment. In this case  $M_{ab}(H) = \chi_{ab}H$  because the sublattice moment continuously rotates towards the field direction. As illustrated in Fig. 2(a),  $H_{c2}^{ab}$  given by Eq. (9) is enhanced by the factor  $1 - \chi_{ab}J_{cf}^{ab}$ . This is compared with the corresponding orbital limit value  $H_{c2}^{ab}(orb) = \alpha_0^{ab}T_{c0}$ . This means that even in the paramagnetic state under suitable conditions, the violation of the Pauli limit is possible, implying that the present violation mechanism is quite generic applicable to other systems. In Fig.2 we summarize the corresponding behaviors for this orientation, and in Fig. 2(c) we schematically plot  $\gamma(H)$  with the Maki parameter  $\mu_M=0.8^{47}$ . Note that the effective field  $H_{eff}(H_{c2}^{ab}) = \alpha_0^{ab}T_{c0}$  is reduced by the factor  $1 - \chi_{ab}J_{cf}^{ab}$  as depicted in Fig. 2(d).

## C. Field tilting from the $c$ -axis to the $ab$ plane

When tilting the field direction from the  $c$ -axis to the  $ab$ -plane by  $\theta$ ,  $H_{c2}(\theta)$  decreases quickly from  $H_{c2}^c=16\text{T}$  to  $H_{c2}(\theta=30^\circ)=4\text{T}^3$ . This finding is analyzed within the present framework. This can be attributed to the angle dependence of the magnetization jump  $M_0(\theta)$  at  $H_{FL}$  as shown in the inset of Fig.3. Namely,  $H_{c2}(\theta)$  is evaluated near the small angle  $\theta$  as

$$H_{c2}(\theta) = \frac{\alpha_0^c}{1 - \chi_c J_{cf}^c} \cdot (T_c(\theta) - T), \quad (12)$$

with  $T_c(\theta) = T_{c0} + \frac{J_{cf}^c}{\alpha_0^c} M_0(\theta)$  for  $H \geq H_{FL}$ . This reduces to Eq. (7) when  $\theta=0$  for the  $c$ -axis. As seen below,  $H_{FL}$  hardly changes with  $\theta$  according to the standard phenomenological theory for the spin flop transition<sup>45</sup>. As will be explained, the AF is quite fragile for the tilted field because the competing two anisotropies;  $K_{AF}(>0)$  aligns the sublattice moment along the  $c$ -axis and  $K$  is the intrinsic anisotropy reflecting the fact that  $\chi_{ab} = 2\chi_c$  in the paramagnetic state<sup>1</sup>. This is characterized by an easy plane XY anisotropy<sup>35</sup>. The spin flop transition is estimated by comparing the two free energies  $f_c$  and  $f_{ab}$  for the AF state with the moment along the  $c$  and  $ab$  directions, respectively. Under the tilted field  $\theta$ , those are given by

$$\begin{aligned} F_c &= -\frac{1}{2}\chi_{ab}\sin^2\theta \cdot H^2 - K_{AF}, \\ F_{ab} &= -\frac{1}{2}\chi_c\cos^2\theta \cdot H^2 - K. \end{aligned} \quad (13)$$

By equalizing the two energies, we obtain

$$H_{FL} = \sqrt{\frac{2(K_{AF} - K)}{\chi_c\cos^2\theta - \chi_{ab}\sin^2\theta}}. \quad (14)$$

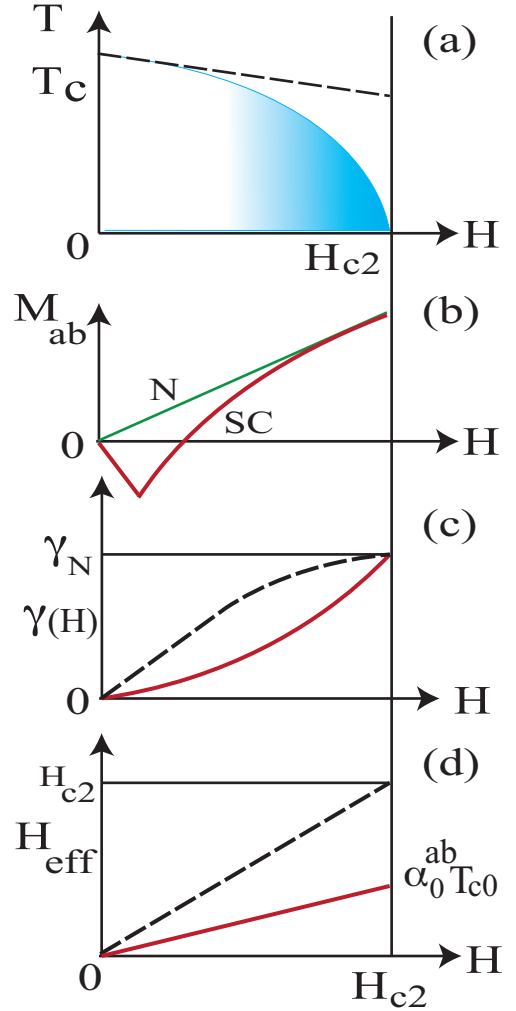


FIG. 2: The field dependences of various quantities for  $H\parallel ab$ -plane. (a)  $H_{c2}^{ab}$  vs  $T$  phase diagram where it is enhanced by  $H_{c2}^{ab}(orb)/(1 - \chi_{ab}J_{cf})$  from the orbital  $H_{c2}^{ab}(orb)$ . The dashed line denotes the initial slope.  $H_{c2}^{ab}(T=0)$  is low because of the paramagnetic effect. (b) Magnetization processes for the normal and SC states. In the normal state  $M_{ab}(H) = \chi_{ab}H$ . In the SC  $M_{ab}(H)$  consists of the superconducting diamagnetic contribution and the paramagnetic contribution due to the localized moments. (c) Field dependence of  $\gamma(H)$ . It shows a strong Pauli affected curve with a concave curvature with  $\mu_M=0.8^{47}$ . The dashed curve indicates  $\gamma(H)$  for the  $s$ -wave case with a full gap without the Pauli paramagnetic effect  $\mu_M = 0^{47}$ . (d) The effective field  $H_{eff}(H) = H$  grows linearly in  $H$  and reaches  $\alpha_0^{ab}T_{c0}$  at  $H_{c2}^{ab}$  far below the unenhanced case drawn by the dashed line.

This reduces to the standard expression<sup>45</sup> of  $H_{FL} = \sqrt{\frac{2(K_{AF}-K)}{\chi_c}}$  when  $\theta=0$ . Equation (14) indicates an absolute instability of the AF with the moment along the  $c$ -axis. This analysis is only meaningful for  $\chi_c\cos^2\theta - \chi_{ab}\sin^2\theta > 0$ , namely,

$$\theta_{cr} \leq \tan^{-1} \sqrt{\chi_c/\chi_{ab}} = \tan^{-1} \sqrt{1/2} = 35.2^\circ. \quad (15)$$

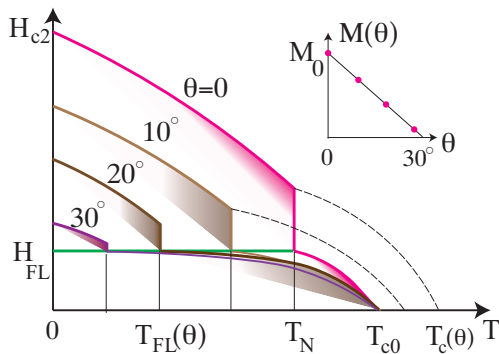


FIG. 3: Angle dependences of  $H_{c2}(\theta)$  where  $\theta$  is the angle from the  $c$ -axis towards the  $ab$ -plane. For  $\theta = 0$ ,  $H_{c2}$  starting from  $T_{c0}$  meets the spin flop transition line denoted by the green line, and it jump vertically around the point at  $(T_N, H_{FL})$ . Then  $H_{c2}$  follows the dashed curve with the enhanced  $T_c(\theta) = T_{c0} + \frac{J_{cf}^c}{\alpha_0^c} M_0(\theta)$  and reaches the enhanced  $H_{c2}(T = 0)$  value given by Eq. (10). Upon increasing  $\theta$  because the initial slopes at  $T_{c0}$  decreases according to the effective mass model,  $T_{FL}(\theta)$  is progressively lowering. Beyond  $\theta > 30^\circ$  it fails to meet the  $H_{FL}$  line denoted by the green horizontal line. Thus no enhanced  $H_{c2}$  occurs. The inset shows the predicted behavior of the magnetization jump  $M_0$  as a function of  $\theta$ .

Beyond  $\theta_{cr}$  the magnetic system may enter the paramagnetic state. Thus it is conceivable that towards this critical angle the jump of the moment  $M_0(\theta)$  decreases. According to our analysis of  $H_{c2}(\theta)$ , we predict that it decreases linearly in  $\theta$  and vanishes around  $\theta_{cr}$ , as shown in the inset of Fig. 3. This can be verified experimentally.

It is noted from Fig. 3 that upon increasing  $\theta$ , (1) As  $M_0(\theta)$  diminishes, the enhanced  $H_{c2}(\theta)$  quickly decreases because  $T_c(\theta)$  given by Eq. (12) drops. (2) While  $H_{FL}$  is nearly independent of  $\theta$ , the first order transition temperature  $T_{FL}(\theta)$  becomes lower because the orbital limit  $H_{c2}^{orb}(\theta) = \alpha(\theta) \cdot (T_{c0} - T)$  with the effective mass  $\alpha(\theta)$  decreases from  $H_{c2}^{orb}(\theta = 0) = 4T$  to  $H_{c2}^{orb}(\theta = 90^\circ) = 2T$  according to the effective mass model discussed later. (3) Thus, above  $\theta \sim 30^\circ$ ,  $H_{c2}(\theta)$  cannot be enhanced simply because  $H_{c2}^{orb}(\theta > 30^\circ)$  is less than  $H_{FL} = 4T$ , namely, it fails to reach the spin flop transition field.

#### D. Pauli paramagnetic effect and $J_{cf}$ values

The orbital limit  $H_{c2}^{orb} = 17T$  and  $= 8T$  for the  $c$  and  $ab$ -axis estimated from their initial slopes at  $T_{c0}$  are suppressed to  $4T$  and  $2T$  respectively<sup>1</sup>. This is because of the Pauli paramagnetic effect signified by the Maki parameter  $\mu_M$ . This  $\mu_M$  is evaluated by employing an empirical formula derived by the microscopic Eilenberger theory<sup>47</sup> based on the effective mass model.

$$H_{c2}(\theta) = \frac{H_{c2}^{orb}(\theta = 90^\circ)}{\sqrt{\Gamma^2 \cos^2 \theta + \sin^2 \theta + 2.4\mu_M^2}}, \quad (16)$$

where  $\Gamma$  is the effective mass anisotropy for the orbital limit  $H_{c2}^{orb}$ . Substituting the above values for the  $c$  and  $ab$ -axes, we determine  $\Gamma = 1.75$  and  $\mu_M = 2.5$ . This large Maki parameter gives rise to the first order transition for ordinary superconductors. Here because of the field scaling  $H_{eff} = (1 - \chi J)H$ , the effective Maki parameter is reduced to  $\mu = (1 - \chi J)\mu_M$  because

$$H_P = \frac{H_P^{BCS}}{1 - \chi J}. \quad (17)$$

For  $H \parallel c$ ,  $\mu_c = 0.4$  and  $(1 - \chi_c J_{cf}^c) = 0.159$ , and for  $H \parallel ab$ ,  $\mu_{ab} = 0.8$  and  $(1 - \chi_{ab} J_{cf}^{ab}) = 0.32$  with  $H_P^{BCS} = 1.84T_{c0} = 0.64T$ . Those moderate Maki parameter values avoid the first order transition at  $H_{c2}$  as observed. We regard that their upper critical fields are both Pauli limited:  $H_P^c = 4.0T$  and  $H_P^{ab} = 2.0T$ . Utilizing the observed susceptibilities<sup>1</sup>  $\chi_c = 0.016\mu_B/T$  and  $\chi_{ab} = 0.029\mu_B/T$ , we obtain  $J_{cf}^c = 52.5T/\mu_B$  and  $J_{cf}^{ab} = 23.4T/\mu_B$ . Their anisotropy  $J_{cf}^c/J_{cf}^{ab} = 2.2$ . This yields the  $H_{c2}$  jump:  $J_{cf}^c M_0 = 52.5 \times \chi_c H_{FL} = 3.6T$  at  $H^c = H_{FL}$ .

#### IV. POSSIBLE APPLICATION TO OTHER MATERIALS

Having performed the detailed analysis on  $CeRh_2As_2$ , we turn to other superconductors that break the Pauli limit to apply the present scenario. As mentioned in Introduction, for the noncentrosymmetric Ce heavy Fermion superconductors<sup>21</sup>,  $CePt_3Si$ ,  $CeIrSi_3$ ,  $CeRhSi_3$  and  $CeCoGe_3$  are possible candidates because (1) our theory requires neither local and global inversion symmetry breaking in the crystalline structure. (2) Because those are all dense Kondo lattice systems, the  $4f$  electrons of the Ce atoms have the dual nature: itinerant and localized characters. In fact, they also exhibit AF order above the superconducting transition, meaning that the  $4f$  electrons of the Ce atoms are localized. (3) The  $cf$  exchange coupling constants  $J_{cf}$  for those systems are expected to be antiferromagnetic, thus the effective field is reduced from the applied external field, enhancing the Pauli limit. Those three conditions satisfy precisely the requirement for the violation of the Pauli limit as explained above.

To facilitate future investigations further, we briefly examine  $CePt_3Si$  with  $T_c = 0.75K$ . As  $H_P^{BCS} = 1.38T$ , the enhancement factor for the  $c$ -axis  $H_{c2}^c(T=0)/H_P^{BCS} = 5T/1.38T = 3.62$ , and thus  $(1 - \chi_c J_{cf}^c) = 0.276$ . By knowing that  $\chi_c = 0.025\mu_B/T$ <sup>23</sup>, we find  $J_{cf}^c = 29.0T/\mu_B$ . Similarly, for the  $ab$ -plane, the corresponding values are  $H_{c2}^{ab}(T=0) = 3T$ , and  $\chi_{ab} = 0.02\mu_B/T$ , which yield  $J_{cf}^{ab} = 23.0T/\mu_B$ . The obtained  $cf$  exchange constants are similar numbers to those of  $CeRh_2As_2$  as mentioned above, suggesting that the same mechanism for the violation of the Pauli limit is working here. The record high  $H_{c2} \sim 45T$  with  $T_c = 2K$  under pressure in  $CeIrSi_3$ <sup>28</sup> may be within our reach although we do not

have further experimental information for the detailed analysis.

It may be interesting to compare the present Kondo systems with the materials where the obvious localized moments embedded in the conduction electrons exert the field compensated internal field through the Jaccarino-Peter mechanism<sup>43</sup>. For example, the Chevrel system  $\text{Eu}_x\text{Sn}_{1-x}\text{Mo}_6\text{S}_8$ <sup>48</sup> has the compensation field  $\sim 30\text{T}$  with the Eu localized moment, giving rise to  $J_{\text{cf}}=8\sim 9\text{T}/\mu_{\text{B}}$ . The exchange constant  $J_{\pi-d}=2.3\mu_{\text{B}}/\text{T}$  in an organic SC:  $\kappa\text{-(BETS)}_2\text{FeBr}_4$  is estimated directly by NMR Knight shift experiment<sup>49</sup>. In this compound the field induced SC is observed around  $15\text{T}$  with  $T_{\text{c}}=0.3\text{K}$ . The present exchange constant  $J_{\text{cf}}$  is an order of magnitude larger than those of non-Kondo materials.

We point out also the case where  $J_{\text{cf}}$  is ferromagnetic in  $\text{TmNi}_2\text{B}_2\text{C}$ <sup>50</sup>. According to the small angle neutron scattering (SANS) experiment<sup>50</sup>, the internal field differs from the applied field because the vortex lattice constant reflects directly the internal field, not applied field. Thus the measurement shows that the internal field is larger than the applied field<sup>50</sup>, indicating that the Tm localized moment *enhances* the applied field by  $\sim 10\%$ , the opposite of the present  $\text{CeRh}_2\text{As}_2$  case. The exchange constant is ferromagnetic. It is understood that heavy Fermion SC is guaranteed for  $J_{\text{cf}}$  to be antiferromagnetic in general, satisfying one of the criteria for the violation of the Pauli limit.

## V. CONCLUSION AND PROSPECTS

As for  $\text{CeRh}_2\text{As}_2$ , it is desirable to perform experiments to better characterize the phase boundary between SC1 and SC2 for  $H\parallel c$  at  $4\text{T}$  because it was interpreted as a spin singlet-triplet pairing change<sup>1-4</sup>. According to our theory, this is nothing but the spin flop transition via a first order. The AF moment is assumed to point to the  $c$ -direction as a fundamental assumption in our theory. This can be verified by various methods, including neutron diffraction experiment. As predicted in Fig. 3 the magnetization jump  $M_0(\theta)$  at  $H_{\text{FL}}=4\text{T}$  vanishes quickly by rotating the applied field from the  $c$ -axis towards the  $ab$ -plane up to  $\theta=30^\circ$ . This is an important prediction to verify our scenario because the enhancement of  $H_{\text{c}2}(\theta)$  near the  $c$ -axis is closely correlated with  $M_0(\theta)$ . Obviously, the gap structure should be characterized more precisely, either full gap or nodal structure. There are several established spectroscopic methods to probe, such as the field-angle dependent specific heat experiment<sup>51</sup>, or the scanning tunneling spectroscopy to probe the local density of states<sup>52,53</sup>.

More generally, apart from  $\text{CeRh}_2\text{As}_2$ , the present theory on the violation mechanism of the Pauli limit can be applied to other SC's, in particular to the Ce containing Kondo systems<sup>21</sup>, including  $\text{CePt}_3\text{Si}$ <sup>22-25</sup>,  $\text{CeIrSi}_3$ <sup>26,27</sup>,

$\text{CeRhSi}_3$ <sup>28</sup> and  $\text{CeCoGe}_3$ <sup>29</sup> as mentioned. Here the duality of the 4f electrons of the Ce atoms is essential where the localized aspect produces the antiferromagnetic exchange field to cancel the applied field, and the itinerant aspect produces the heavy Fermions. Both aspects are crucial to attain the high field superconductivity beyond the Pauli-Clogston limit. The extremely enhanced  $H_{\text{c}2}$  observed in those materials largely remains unexplained so far. We propose several experiments on these superconductor to establish the generality of our idea on the violation mechanism: (1) To probe the actual internal field, or magnetic induction, which is a non-trivial task, the Knight shift experiment of NMR is one of the direct methods. In fact, it is applied successfully to probe the compensation field in the organic superconductor<sup>49</sup>. (2) As mentioned above, the SANS experiment is also powerful to verify the internal field because the vortex lattice spacing directly reflects the internal field via the flux quantization rule<sup>50</sup>.

We should point out a common and unexpected feature between two singlet and triplet superconductors where both are driven and reinforced by the incipient magnetization; The  $H_{\text{c}2}$  enhancement in a spin singlet pairing here is analogous to the physics<sup>54-56</sup> in spin triplet pairing in a series of magnetically polarized superconductors:  $\text{UGe}_2$ ,  $\text{URhGe}$ ,  $\text{UCoGe}$ , and  $\text{UTe}_2$ , where the field reinforced  $H_{\text{c}2}$  is observed. While the magnetization  $M(H)$  is coupled through the exchange interaction  $J_{\text{cf}}$  in the form  $M(H)J_{\text{cf}}$  on the conduction electrons in a singlet case, it directly couples with a triplet pairing vectorial order parameter  $\vec{\eta}$  in the form of  $\kappa\vec{M}(H)\cdot\vec{\eta}\times\vec{\eta}^*$ . This common field-reinforced SC feature is deeply rooted in the duality nature of the f-electrons, itinerant and localized.

Finally, it should be noticed that the present mechanism of the Pauli-Clogston limit violation has been applied so far to the spin singlet pairing case in mind, but it can work in the spin triplet pairing as well without any alternation. Thus, it might be interesting to verify whether or not the observed extremely high  $H_{\text{c}2}$  enhancement over the Pauli limit;  $60\text{T}/1.84T_{\text{c}}\sim 22$  in  $\text{UTe}_2$  with  $T_{\text{c}}=1.5\text{K}$  needs this mechanism in addition to the spin triplet pairing symmetry.

## Acknowledgments

The author sincerely thanks K. Ishida and S. Kitagawa for enlightening discussions and for sharing the data before publication, which were crucial for forming the present idea, and T. Sakakibara and Y. Machida for their help in widening the scopes of the present theory. The author is indebted to Editage for English language editing. This work is supported by JSPS-KAKENHI, No. 17K05553 and No.21K03455.

- <sup>1</sup> S. Khim, J. F. Landaeta, J. Banda, N. Bannor, M. Brando, P. M. R. Brydon, D. Hafner, R. K uchler, R. Cardoso-Gil, U. Stockert, A. P. Mackenzie, D. F. Agterberg, C. Geibel, and E. Hassinger, Field-induced transition from even to odd parity superconductivity in CeRh<sub>2</sub>As<sub>2</sub>. *Science* **373**, 1012 (2021).
- <sup>2</sup> D. Hafner, P. Khanenko, E. -O. Eljaouhari, R. K uchler, J. Banda, N. Bannor, T. L uhmann, J. F. Landaeta, S. Mishra, I. Sheikin, E. Hassinger, S. Khim, C. Geibel, G. Zwicknagl, and M. Brando, Possible quadrupole density wave in the superconducting Kondo lattice CeRh<sub>2</sub>As<sub>2</sub>. *Phys. Rev. X* **12**, 011023 (2022).
- <sup>3</sup> J. F. Landaeta, P. Khanenko, D. C. Cavanagh, C. Geibel, S. Khim, S. Mishra, I. Sheikin, P. M. R. Brydon, D. F. Agterberg, M. Brando, and E. Hassinger, Field-angle dependence reveals odd-parity superconductivity in CeRh<sub>2</sub>As<sub>2</sub>. *Phys. Rev. X* **12**, 031001 (2022).
- <sup>4</sup> S. Onishi, U. Stockert, S. Khim, J. Banda, M. Brando, and E. Hassinger, Low-temperature thermal conductivity of the two-phase superconductor CeRh<sub>2</sub>As<sub>2</sub>. *Frontiers in Electronic Materials*, **2**, 880579 (2022).
- <sup>5</sup> S. Kimura, J. Sichelshmidt, and S. Khim, Optical study on electronic structure of the locally non-centrosymmetric CeRh<sub>2</sub>As<sub>2</sub>. arXiv:2109.00758.
- <sup>6</sup> Eric G. Schertenleib, Mark H. Fischer, and Manfred Sigrist, Unusual H-T phase diagram of CeRh<sub>2</sub>As<sub>2</sub>: The role of staggered noncentrosymmetry, *Phys. Rev. Research* **3**, 023179 (2021).
- <sup>7</sup> David M ockli and Aline Ramires, Two scenarios for superconductivity in CeRh<sub>2</sub>As<sub>2</sub>. *Phys. Rev. Research* **3**, 023204 (2021).
- <sup>8</sup> Andrzej Ptok, Konrad J. Kapcia, Pawel T. Jochym, Jan La zewski, Andrzej M. Ole , and Przemyslaw Piekarczyk, Electronic and dynamical properties of CeRh<sub>2</sub>As<sub>2</sub>: Role of Rh<sub>2</sub>As<sub>2</sub> layers and expected orbital order. *Phys. Rev. B* **104**, L041109 (2021).
- <sup>9</sup> David M ockli and Aline Ramires, Superconductivity in disordered locally noncentrosymmetric materials: An application to CeRh<sub>2</sub>As<sub>2</sub>. *Phys. Rev. B* **104**, 134517 (2021).
- <sup>10</sup> D. C. Cavanagh, T. Shishidou, M. Weinert, P. M. R. Brydon, and Daniel F. Agterberg. Nonsymmorphic symmetry and field-driven odd-parity pairing in CeRh<sub>2</sub>As<sub>2</sub>. *Phys. Rev. B* **105**, L020505 (2022).
- <sup>11</sup> Tamaghna Hazra and Piers Coleman, Triplet pairing mechanisms from Hund's-Kondo models: applications to UTe<sub>2</sub> and CeRh<sub>2</sub>As<sub>2</sub>. arXiv:2205.13529 (2022).
- <sup>12</sup> Kosuke Nogaki, and Youichi Yanase, Even-odd parity transition in strongly correlated locally noncentrosymmetric superconductors: An application to CeRh<sub>2</sub>As<sub>2</sub>. arXiv:2206.04288.
- <sup>13</sup> Eric G. Schertenleib, Mark H. Fischer, and Manfred Sigrist, Unusual H-T phase diagram of CeRh<sub>2</sub>As<sub>2</sub>: The role of staggered noncentrosymmetry, *Phys. Rev. Research* **3**, 023179 (2021).
- <sup>14</sup> Ernst Bauer and Manfred Sigrist, Non-centrosymmetric superconductors: introduction and overview, Vol. 847 (Springer Science and Business Media, 2012).
- <sup>15</sup> Mark H. Fischer, Florian Loder, and Manfred Sigrist, Superconductivity and local noncentrosymmetry in crystal lattices. *Phys. Rev. B* **84**, 184533 (2011).
- <sup>16</sup> Daisuke Maruyama, Manfred Sigrist, and Youichi Yanase, Locally non-centrosymmetric superconductivity in multilayer systems. *J. Phys. Soc. Jpn.*, **81**, 034702 (2012).
- <sup>17</sup> Tomohiro Yoshida, Manfred Sigrist, and Youichi Yanase, Pair-density wave states through spin-orbit coupling in multilayer superconductors, *Phys. Rev. B* **86**, 134514 (2012).
- <sup>18</sup> Tomohiro Yoshida, Manfred Sigrist, and Youichi Yanase, Complex-stripe phases induced by staggered Rashba spin-orbit coupling. *J. Phys. Soc. Jpn.*, **82**, 074714 (2013).
- <sup>19</sup> Tomohiro Yoshida, Manfred Sigrist, and Youichi Yanase, Parity-mixed superconductivity in locally non-centrosymmetric system. *J. Phys. Soc. Jpn.*, **83**, 013703 (2014).
- <sup>20</sup> Tomohiro Yoshida, Manfred Sigrist, and Youichi Yanase, Topological crystalline superconductivity in locally non-centrosymmetric multilayer superconductors. *Phys. Rev. Lett.* **115**, 027001 (2015).
- <sup>21</sup> C. Pfleiderer, Superconducting phase of f-electron compounds, *Rev. Mod. Phys.* **81**, 1551 (2009).
- <sup>22</sup> E. Bauer, G. Hilscher, H. Michor, Ch. Paul, E. W. Scheidt, A. Gribanov, Yu. Seropegin, H. No l, M. Sigrist, and P. Rogl, Heavy Fermion Superconductivity and Magnetic Order in Noncentrosymmetric CePt<sub>3</sub>Si. *Phys. Rev. Lett.*, **92**, 027003 (2004).
- <sup>23</sup> T. Takeuchi, S. Hashimoto, T. Yasuda, H. Shishido, T. Ueda, M. Yamada, Y. Obiraki, M. Shiimoto, H. Kohara, T. Yamamoto, K. Sugiyama, K. Kindo, T. D. Matsuda, Y. Haga, Y. Aoki, H. Sato, R. Settai, and Y. Onuki, Magnetism and superconductivity in a heavy-fermion superconductor, CePt<sub>3</sub>Si. *J. Phys.: Condens. Matter*, **16**, L333-L342 (2004).
- <sup>24</sup> N. Metoki, K. Kaneko, T. D. Matsuda, A. Galatanu, T. Takeuchi, S. Hashimoto, T. Ueda, R. Settai, Y. Onuki, and N. Bernhoeft, Magnetic structure and the crystal field excitation in heavy-fermion antiferromagnetic superconductor CePt<sub>3</sub>Si. *J. Phys.: Condens. Matter*, **16**, L207-L212 (2004).
- <sup>25</sup> M. Yagi, H. Mukuda, Y. Kitaoka, S. Hashimoto, T. Yasuda, R. Settai, T. D. Matsuda, Y. Haga, Y. Onuki, P. Rogl, and E. Bauer, Evidence for novel pairing state in noncentrosymmetric superconductor CePt<sub>3</sub>Si: <sup>29</sup>Si-NMR Knight shift study. *J. Phys. Soc. Jpn.*, **75**, 013709 (2006).
- <sup>26</sup> H. Mukuda, T. Ohara, M. Yashima, Y. Kitaoka, R. Settai, Y. Onuki, K. M. Itoh, and E. E. Haller, Spin Susceptibility of Noncentrosymmetric Heavy-Fermion Superconductor CeIrSi<sub>3</sub> under Pressure: <sup>29</sup>Si Knight-Shift Study on Single Crystal. *Phys. Rev. Lett.*, **104**, 017002 (2010).
- <sup>27</sup> R. Settai, K. Katayama, D. Aoki, I. Sheikin, G. Knebel, J. Flouquet, and Y. Onuki, Field-Induced Antiferromagnetic State in Non-centrosymmetric Superconductor CeIrSi<sub>3</sub>. *J. Phys. Soc. Jpn.*, **80**, 094703 (2011).
- <sup>28</sup> N. Kimura, K. Ito, H. Aoki, S. Uji, and T. Terashima, Extremely High Upper Critical Magnetic Field of the Non-centrosymmetric Heavy Fermion Superconductor CeRhSi<sub>3</sub>. *Phys. Rev. Lett.*, **98**, 197001 (2007).
- <sup>29</sup> R. Settai, Y. Okuda, I. Sugitani, Y. Onuki, T. D. Matsuda, Y. Haga, and H. Harima, Non-centrosymmetric heavy Fermion superconductivity in CeCoGe<sub>3</sub>. *Int. J. Mod. Phys. B* **21**, 3238 (2007).
- <sup>30</sup> Kenta M. Suzuki, Kazushige Machida, Yasumasa Tsutsumi, and Masanori Ichioka, Microscopic Eilenberger the-

- ory of Fulde-Ferrell-Larkin-Ovchinnikov states in the presence of vortices. *Phys. Rev. B* **101**, 214516 (2020).
- <sup>31</sup> J. M. Lu, O. Zheliuk, L. Leermakers, N. F. Q. Yuan, U. Zeitler, K. T. Law and J. T. Ye, Evidence for two-dimensional Ising superconductivity in gated MoS<sub>2</sub>, *Science*, **350**, 11353 (2015).
- <sup>32</sup> Y. Sato, Y. Kasahara, J. Ye, Y. Iwasa, and T. Nojima, Metallic ground state in an ion-gated two-dimensional superconductor. *Science*, **350**, 409 (2015).
- <sup>33</sup> Yuan Cao, Jeong Min Park, Kenji Watanabe, Takashi Taniguchi, Pablo Jarillo-Herrero, Large Pauli Limit Violation and Reentrant Superconductivity in Magic-Angle Twisted Trilayer Graphene. arXiv:2103.12083.
- <sup>34</sup> M. Kibune, S. Kitagawa, K. Kinjyo, S. Ogata, M. Manago, T. Taniguchi, K. Ishida, M. Brando, E. Hassinger, H. Rosner, C. Geibel, and S. Khim, Observation of antiferromagnetic order as odd-parity multipoles inside the superconducting phase in CeRh<sub>2</sub>As<sub>2</sub>. *Phys. Rev. Lett.*, **128**, 057002 (2022).
- <sup>35</sup> S. Kitagawa, M. Kibune, K. Kinjyo, M. Manago, T. Taniguchi, K. Ishida, M. Brando, E. Hassinger, H. Rosner, C. Geibel, and S. Khim, Two-dimensional XY-type magnetic properties of local noncentrosymmetric superconductor CeRh<sub>2</sub>As<sub>2</sub>. *J. Phys. Soc. Jpn.*, **91**, 043702 (2022).
- <sup>36</sup> S. Ogata, M. Kibune, K. Kinjyo, S. Kitagawa, K. Ishida, M. Brando, E. Hassinger, H. Rosner, C. Geibel, and S. Khim, NMR study in the superconducting multiphase of the locally inversion breaking heavy fermion superconductor CeRh<sub>2</sub>As<sub>2</sub>. 77th Annual Meeting of Japan Physical Society, 17aGB33-4 (2022).
- <sup>37</sup> K. Ishida, private communication.
- <sup>38</sup> J. F. Landaeta, A. M. Leon, S. Zwickel, T. Lühmann, M. Brando, C. Geibel, E. -O. Eljaouhari, H. Rosner, G. Zwicknagl, E. Hassinger, and S. Khim, Conventional type-II superconductivity in locally non-centrosymmetric LaRh<sub>2</sub>As<sub>2</sub> single crystals. *Phys. Rev. B* **106** 014506 (2022).
- <sup>39</sup> K. Machida and H. Nakanishi, Superconductivity under a ferromagnetic molecular field. *Phys. Rev. B* **30** 122 (1984).
- <sup>40</sup> K. Machida, K. Nokura, and T. Matsubara, Theory of antiferromagnetic superconductors. *Phys. Rev. B* **22**, 2307 (1980).
- <sup>41</sup> K. Machida and T. Matsubara, Spin Density Wave and Superconductivity in Highly Anisotropic Materials. II. Detailed Study of Phase Transitions. *J. Phys. Soc. Jpn.* **50**, 3231 (1981).
- <sup>42</sup> K. Machida and M. Kato, Inherent spin-density-wave instability in heavy Fermion superconductivity. *Phys. Rev. Lett.* **58**, 1986 (1987).
- <sup>43</sup> V. Jaccarino and M. Peter, Ultra-high-field superconductivity. *Phys. Rev. Lett.* **9**, 290 (1962).
- <sup>44</sup> S. Araki, N. Metoki, A. Galatanu, E. Yamamoto, A. Thamizhavel, and Y. Ōnuki, Crystal structure, magnetic ordering, and magnetic excitation in the 4f-localized ferromagnet CeAgSb<sub>2</sub>. *Phys. Rev. B* **68**, 024408 (2003).
- <sup>45</sup> J. Kanamori, in *Magnetism* vol. I, edited by G. T. Rado and H. Suhl, Academic Press 1963.
- <sup>46</sup> M. Ichioka and K. Machida, Vortex states in superconductors with strong Pauli-paramagnetic effect. *Phys. Rev. B* **76**, 064502 (2007).
- <sup>47</sup> K. Machida and M. Ichioka, Magnetic field dependence of low-temperature specific heat in Sr<sub>2</sub>RuO<sub>4</sub>. *Phys. Rev. B* **77**, 184515 (2008).
- <sup>48</sup> H. W. Meul, C. Rossel, M. Decroux, Ø. Fischer, G. Remeinyi, and A. Briggs, Observation of magnetic-field-induced superconductivity. *Phys. Rev. Lett.*, **53**, 497 (1984).
- <sup>49</sup> S. Fujiyama, M. Takigawa, J. Kikuchi, H.-B. Cui, H. Fujiwara, and H. Kobayashi, Compensation of Effective Field in the Field-Induced Superconductor  $\kappa$ -(BETS)<sub>2</sub>FeBr<sub>4</sub> Observed by <sup>77</sup>Se NMR. *Phys. Rev. Lett.*, **96**, 217001 (2006).
- <sup>50</sup> L. DeBeer-Schmitt, M. R. Eskildsen, M. Ichioka, K. Machida, N. Jenkins, C. D. Dewhurst, A. B. Abrahamson, S. L. Bud'ko, and P. C. Canfield, Pauli Paramagnetic Effects on Vortices in Superconducting TmNi<sub>2</sub>B<sub>2</sub>C. *Phys. Rev. Lett.*, **99**, 167001 (2007).
- <sup>51</sup> P. Miranović, N. Nakai, M. Ichioka, and K. Machida, Orientational field dependence of low-lying excitations in the mixed state of unconventional superconductors. *Phys. Rev. B* **68**, 052501 (2003).
- <sup>52</sup> N. Hayashi, M. Ichioka, and K. Machida, Star-shaped local density of states around vortices in a type II superconductor. *Phys. Rev. Lett.*, **77**, 4074 (1996).
- <sup>53</sup> M. Ichioka, and K. Machida, Local density of states in the vortex lattice in a type II superconductor. *Phys. Rev. B* **55**, 6565 (1997).
- <sup>54</sup> K. Machida, Theory of Spin-polarized Superconductors—An Analogue of Superfluid <sup>3</sup>He A-phase—. *J. Phys. Soc. Jpn.* **89**, 033702 (2020).
- <sup>55</sup> K. Machida, Notes on Multiple Superconducting Phases in UTe<sub>2</sub> –Third Transition—. *J. Phys. Soc. Jpn.* **89**, 065001 (2020).
- <sup>56</sup> K. Machida, Nonunitary triplet superconductivity tuned by field-controlled magnetization: URhGe, UCoGe, and UTe<sub>2</sub>. *Phys. Rev. B* **104**, 014514 (2021).